Electronic Supplementary Material (ESI) for CrystEngComm.

Supporting Information

Crystalline Packing in Pentacene-like Organic Semiconductors

Michael Klues and Gregor Witte*

Fachbereich Physik, Philipps-Universität Marburg, Renthof 7, 35032 Marburg, Germany.
E-Mail: gregor.witte@physik.uni-marburg.de

Table of Contents

Abbreviations. All abbreviation used within the supporting information are listed below and are in accordance with the notation used in the article.

Molecules:

DAP	Diazapentacene
DHDAP	Dihydrodiazapentacene
DNTT	Dinaphthothienothiophene
HFDP	Hexafluorodiazapentacene
PEN	Pentacene
PFP	Perfluoropentacene
QUA	Quinacridone
QUI	Pentacenequinone
TET	Pentacenetetrone

Polymorphs:

PEN-C	Pentacene Campbell Phase
PEN-S	Pentacene Siegrist Phase
PEN-TF	Pentacene Thin Film Phase
PFP-bulk	Perfluoropentacene Bulk Phase
PFP-π	Perfluoropentacene π-stacked Phase
QUA-α	Quinacridone α-Phase
QUA-β	Quinacridone β-Phase
QUA-γ	Quinacridone γ-Phase

Table ST1: Crystal structure data. Abbreviations for packing motifs: HB = Herringbone, SS = Slip-Stack, CC = Criss-Cross. For QUA-α and QUI the assignment to one of the motifs is not unique.

Structure	a [Å]	b [Å]	c [Å]	α [°]	β [°]	γ [°]	Z	Space Group	Packing Motif	Ref.
PEN-C	7.90	6.06	16.01	101.9	112.6	85.8	2	P1	HB	[1]
PEN-S	6.27	7.79	14.51	76.65	87.50	84.61	2	P1	HB	[2]
PEN-TF	5.96	7.60	15.61	81.25	86.56	89.80	2	P1	HB	[3]
PFP-bulk	15.51	4.49	11.45	90.00	91.57	90.00	2	$P2_1/c$	HB	[4]
PFP-π	15.13	8.94	6.51	78.56	108.14	92.44	2	P1	SS	[5]
DNTT	6.19	7.66	16.21	90.00	92.49	90.00	2	$P2_1$	HB	[6]
QUA-α	3.80	6.61	14.49	100.69	94.41	102.11	1	P1	SS	[7]
QUA-β	5.69	3.98	30.02	90.00	96.77	90.00	2	$P2_1/c$	SS / CC	[7]
QUA-γ	13.70	3.88	13.40	90.00	100.44	90.00	2	$P2_1/c$	CC	[7]
QUI	4.95	17.78	8.17	90.00	90.00	93.26	2	$P2_1/b$	SS / CC	[8, 9]
TET	4.71	7.48	11.08	97.86	93.85	99.37	1	P1	SS	[9]
DHDAP	5.75	8.88	13.17	87.44	84.84	86.22	2	P1	HB	[10]
DAP	13.17	5.20	9.93	90.00	100.00	90.00	2	$P2_1/a$	CC	[11,12]
HFDP	12.37	8.08	14.39	90.00	93.76	90.00	4	$P2_1/c$	CC	[13]

The crystal structure of pentacenequinone (QUI) originally was determined by Dzyabchenko *et al.* [8], but for the Hirshfeld analysis within this study data from reference [9] were used. Also a thin-film polymorphism is known [14], this structure is not included within this study because the structural change is comparable to the case of PEN-TF. Molecules arrange more upright to maximize interactions with the surface. Interestingly this furthermore leads to a slight change of the packing motif which is of SS type within the thin film phase. This behavior is comparable to the case of QUA-α and QUA-β. For clarity this redundant example was left out.

[1] R.B. Campbell and J.M. Robertson, *Acta Cryst*., 1962, **15**, 289.
[2] T. Siegrist, C. Kloc, J.H. Schön, B. Batlogg, R.C. Haddon, S. Berg and G.A. Thomas, *Angew. Chem. Int. Ed*., 2001, **40**, 1732.
[3] S. Schiefer, M. Huth, A. Dobrinevski and B. Nickel, *J. Am. Chem. Soc.*, 2007, **129**, 10316.
[4] Y. Sakamoto, T. Suzuki, M. Kobayashi, Y. Gao, Y. Fukai, Y. Inoue, F. Sato, S. Tokito, *J. Am. Chem. Soc*. 2004, **126**, 8138.
[5] I. Salzmann, A. Moser, M. Oehzelt, T. Breuer, X. Feng, Z.Y. Juang, D. Nabok, R.G. Della Valle, S. Duhm, G. Heimel, A. Brillante, E. Venuti, I. Bilotti, C. Christodoulou, J. Frisch, P. Puschnig, C. Draxl, G. Witte, K. Müllen and N. Koch, *ACS Nano*, 2012, **6**, 10874.
[6] T. Yamamoto and K. Takimiya, *J. Am. Chem. Soc*., 2007, **129**, 2224.
[7] E.F. Paulus, F.J.J. Leusen, and M.U. Schmidt, *CrystEngComm*, 2007, **9**, 131.
[8] A.V. Dzyabchenko, V.E. Zavodnik and V.K. Belsky, *Acta Cryst. B*, 1979, **35**, 2250.
[9] D. Käfer, M. El Helou, C. Gemel, G. Witte, *Cryst. Growth Design* 2008, **8**, 3053.
[10] Q. Tang, D.Q. Zhang, S.L. Wang, N. Ke, J.B. Xu, J.C. Yu, Q. Miao, *Chem. Mater*. 2009, **21**, 1400.
[11] D. Liu, Z. Li, Z. He, J. Xu and Q. Miao, *J. Mater. Chem.*, 2012, **22**, 4396.
[12] Q. Miao, *Synlett*. 2012, **3**, 326.
[13] J. Schwaben, N. Münster, M. Klues, T. Breuer, P. Hofmann, K. Harms, G. Witte, U. Koert, *Chem. Eur. J*. 2015, **21**, 13758.
[14] I. Salzmann, D. Nabok, M. Oehzelt, S. Duhm, A. Moser, G. Heimel, P. Puschnig, C. Ambrosch-Draxl, J. P. Rabe and N. Koch, *Cryst. Growth Des.*, 2011, **11,** 600.

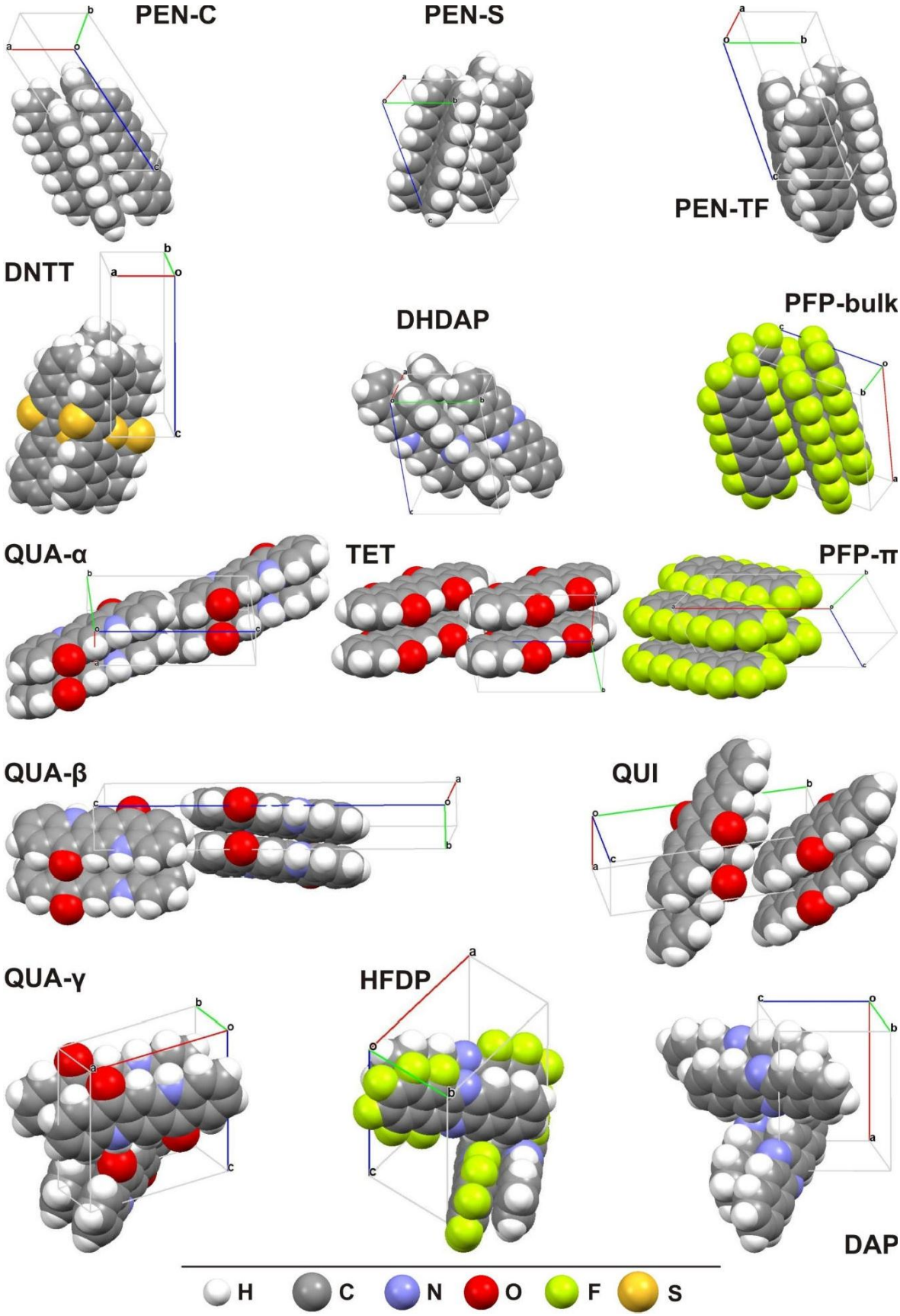

Figure S1: Visualization of packing motifs for all considered crystal structures together with the unit cells. The bottom line displays the color code used for representation of the various atoms.

Annotations related to the Hirshfeld surface

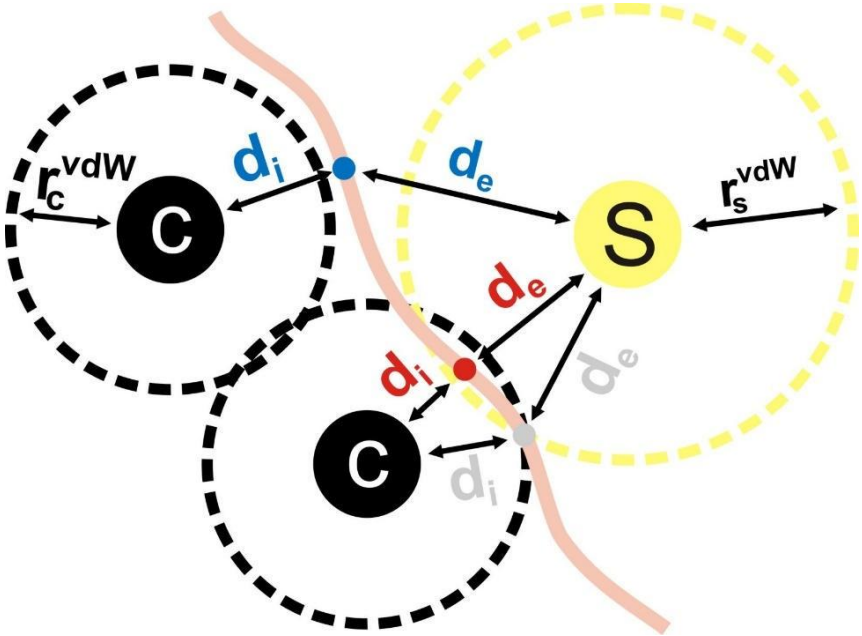

Figure S2: Illustration of distances and colors for fingerprint plots and the d_{norm} color-code.

Figure S2 depicts two carbon atoms, which are part of a molecule, as well as a sulfur atom, which is part of a neighboring molecule. These atoms - or more precise - the molecules they are part of, are separated by a Hirshfeld-surface, indicated as pink line in-between. Assuming the carbon atoms to be located within the Hirshfeld-volume, surrounded by the corresponding surface a pair of d_i- and d_e-values can be found for every point of the surface. These values are defined as the distances to the next atom interior (d_i) and exterior (d_e) to the Hirshfeld-volume. Plotting these numbers against each other and color coding their occurrence, as discussed in the article, leads to fingerprint plots. Due to the fact, that the connecting line between an atom inside and another one outside the volume always intersects the surface the close contacts are also encoded in the fingerprint plots (red point in Fig. S1). The close contact distance is simply the sum of the corresponding d_i- and d_e-values. Furthermore, these values can also be used to generate the d_{norm}. Therefore, the distances are related to the van der Waals radii of the corresponding atoms (dashed circles in fig. S1). Whenever distances and radii equal each other the surface is colored in gray shades, while red indicates intersections with neighboring van der Waals spheres and blue the absence of such intersections. Hence red areas on the surface can denote regions of strong intermolecular interaction. Interestingly close contacts do not necessarily lead to a red region on the surface due to the dependence on the vdW-radii. Thus, the d_{norm} gives element specific contact points between molecules.

Element specific fingerprint plots

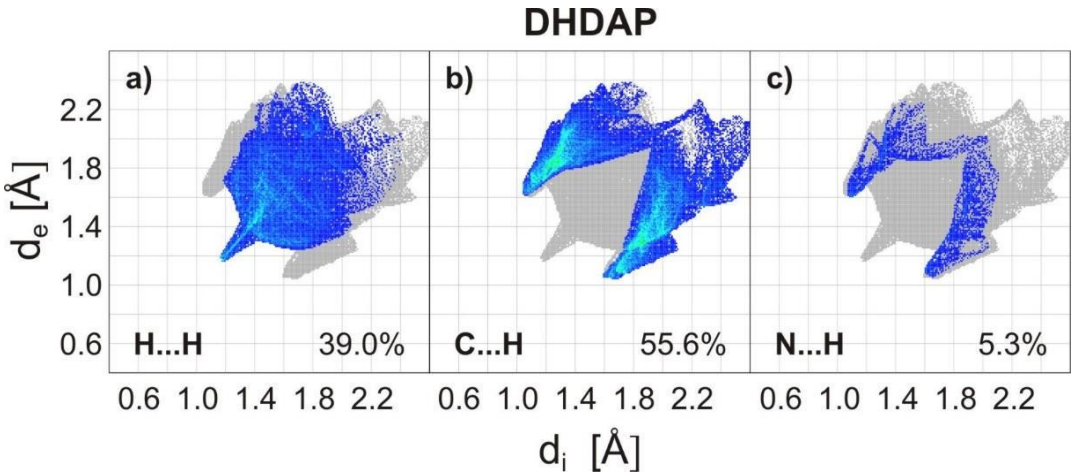

Figure S3: Element specific fingerprint plots for DHDAP. All atom combinations including hydrogen are shown because these cases cover 99.9% of the Hirshfeld surface. Fingerprint plots of heteroatomic combinations always include also the mirrored case, e.g. C…H=C…H+H…C.

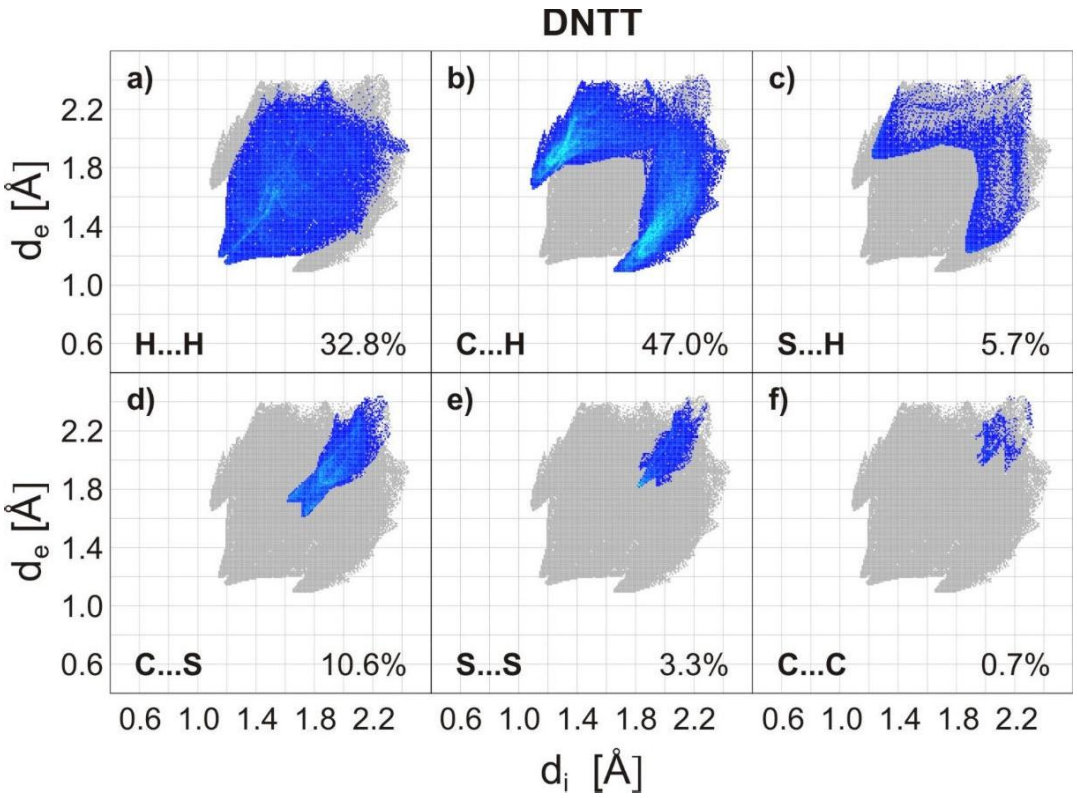

Figure S4: Element specific fingerprint plots for DNTT. All possible atom combinations are considered. Fingerprint plots of heteroatomic combinations always include also the mirrored case, e.g. C…H=C…H+H…C.

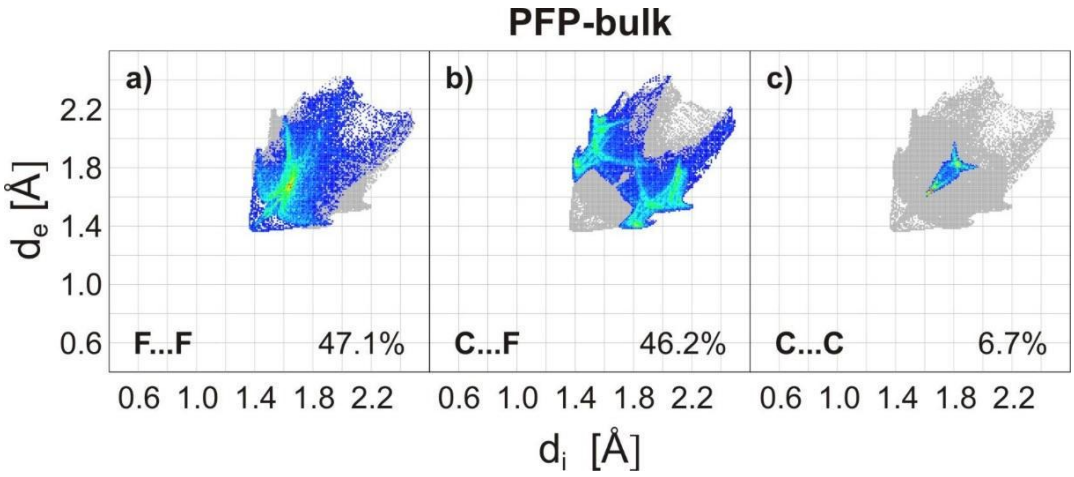

Figure S5: Element specific fingerprint plots for PFP-bulk. All possible atom combinations are considered. Fingerprint plots of heteroatomic combinations include also the mirrored case, e.g. C…F=C…F+F…C.

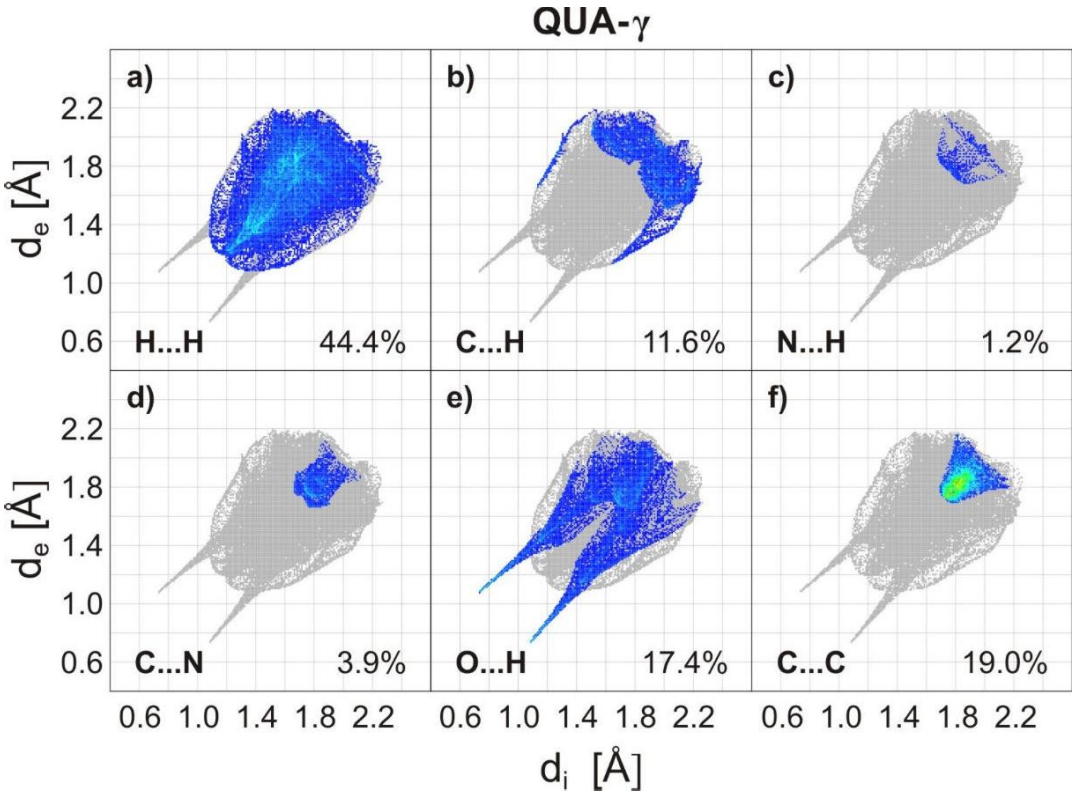

Figure S6: Element specific fingerprint plots for QUA-γ. Most significant atom combinations are considered. Fingerprint plots of heteroatomic combinations always include also the mirrored case, e.g. C…H=C…H+H…C.

Atomic Distances

Fingerprint plots are also used to determine distances between adjacent atoms. Element specific fingerprint plots allow to identify the smallest sum of a d_i-d_e pair. This approach yields the same values as directly measuring close contacts between two neighboring atoms, since the corresponding connecting line needs to intersect the Hirshfeld surface, which necessarily yields a d_i-d_e pair for this smallest distance. Note that this definition is also applied to the C…C contacts. Therefore, the presented values don`t implicitly represent the molecular plane distance, which should be systematically smaller than the given numbers, but are nevertheless quite close to the plane distances.

*Table ST2: Close contact distances for different atom pairs. Values labeled with * are given for completeness, but corresponding fingerprint plots do not show distinct features, indicating interactions mediated by this atom pairs.*

	C…H (Å)	N…H (Å)	O…H (Å)	F…H (Å)	C…F (Å)	C…C (Å)	H…H (Å)	F…F (Å)	C…S (Å)
PEN-C	2.73						2.32*		
PEN-S	2.82						2.36*		
PEN-TF	2.81						2.36*		
DNTT	2.73						2.34		3.30
DAP	2.76	2.48				3.50	2.17		
DHDAP	2.65	2.68					2.34		
HFDP		2.68		2.68	3.04	3.32	2.76*	2.66	
QUI			2.53			3.50	2.34		
TET			2.31			3.36	2.62		
QUA-α			1.78			3.38	1.72		
QUA-β			1.90			3.40	2.06		
QUA-γ			1.81			3.43	2.32		
PFP-bulk					3.10	3.22		2.74	
PFP-π					2.96	3.18		2.76	

Correlation Coefficients

All correlation coefficients have been calculated according to the definition of Spearman and Pearson [1] for fingerprints with 15x15 bins and a scale of 0 to 3Å. Calculations were performed using python standard routines. [2]

Table ST3: Correlation coefficients for fingerprints of all crystal structures.

	DNTT	DHDAP	PEN-S	PEN-C	PEN-TF	PFP-bulk	PFP-π	QUA-β	QUA-α	QUA-γ	DAP	QUI	HFDP	TET
DNTT	1.0	0.77	0.84	0.87	0.88	0.61	0.61	0.61	0.58	0.59	0.7	0.69	0.66	0.7
DHDAP		1.0	0.96	0.94	0.91	0.53	0.5	0.57	0.44	0.45	0.65	0.6	0.56	0.55
PEN-S			1.0	0.96	0.96	0.56	0.52	0.61	0.48	0.51	0.66	0.63	0.59	0.59
PEN-C				1.0	0.97	0.56	0.5	0.62	0.46	0.51	0.66	0.64	0.59	0.61
PEN-TF					1.0	0.53	0.51	0.6	0.48	0.48	0.62	0.6	0.57	0.58
PFP-bulk						1.0	0.95	0.67	0.71	0.64	0.61	0.72	0.85	0.82
PFP-π							1.0	0.64	0.69	0.63	0.62	0.73	0.84	0.82
QUA-β								1.0	0.87	0.87	0.8	0.86	0.8	0.79
QUA-α									1.0	0.93	0.82	0.87	0.84	0.82
QUA-γ										1.0	0.85	0.88	0.82	0.8
DAP											1.0	0.91	0.82	0.79
QUI												1.0	0.89	0.91
HFDP													1.0	0.9
TET														1.0

[1] A. Parkin, G. Barr, W. Dong, C. J. Gilmore, D. Jayatilaka, J.J. MacKinnon, M.A. Spackman and C.C. Wilson, *CrystEngComm*, 2007, **9**, 648.
[2] Python Software Foundation. Python Language Reference, version 2.7.6. Available at http://www.python.org

Thin film phase of QUI

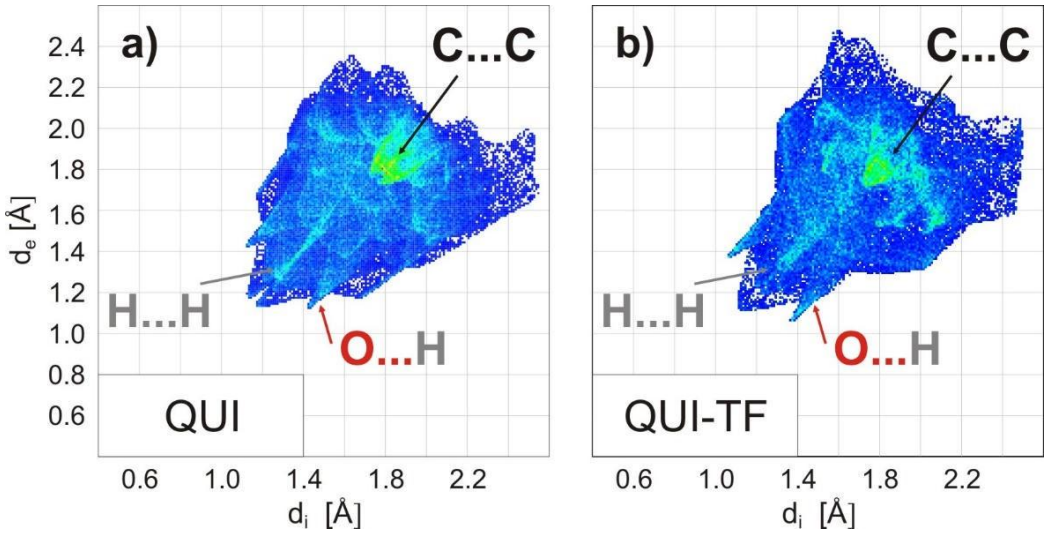

Figure S7: Fingerprint plots of the QUI-bulk structure a) and the thin film phase b) [1].

[1] I. Salzmann, D. Nabok, M. Oezelt, S. Duhm, A, Moser, G. Heimel, P. Puschnig, C. Ambrosch-Draxl, J.P. Rabe, N. Koch, Cryst. Growth Des. 11, 601 (2011).

Computing Molecular Properties

All properties were calculated with the US-GAMESS code [1], using DFT with the B3LYP functional and a 6311G(d,p) basis set. Molecules were at first geometry optimized by considering their symmetry before calculation of their polarizabilities and quadrupole moments. The precision of polarizability calculations was improved by decreasing convergence criteria, primitive cutoff factors as well as integral cutoffs. Energy and dipole derived polarizabilities are found to be equal for all molecules up to the fourth significant digit. Molecules were placed parallel to the xy-plane with their symmetry center at the origin, so that the z-axis is perpendicular to the molecular plane. The long axis of the molecules is oriented along the x-direction and therefore the short axis of the molecules is parallel to the y-axis. DNTT is an exception since in this case a long axis is not clearly defined. Here the long axis of the naphthalene subunits was oriented in x-direction. Due to symmetry reasons, this orientation directly yields diagonal polarizability and quadrupole tensors for all molecules except DNTT and QUA. In these cases, the tensor was diagonalized to provide better comparability. For the polarizability tensors this is a minor manipulation since diagonalization can be obtained by a rotation around the z-axis of less than 5 degrees in both cases, while for the quadrupole tensor rotations of 12 degrees for DNTT and 30 degrees for QUA are needed.

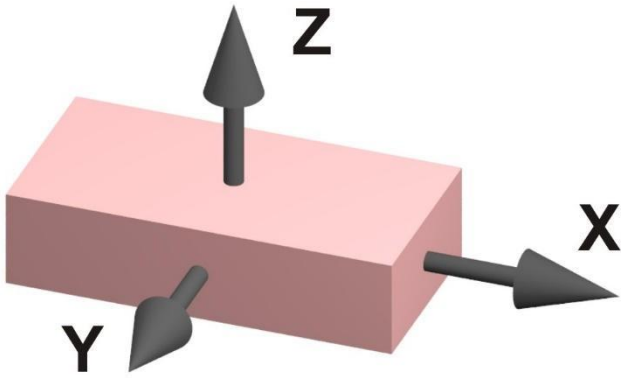

Figure S8: General orientation of molecules within the coordinate system for calculations.

[1] http://www.msg.ameslab.gov/gamess

Polarizability:

Table ST4: Computed α-polarizability of all molecules in $10^{-24}cm^3$. Static dipole polarizability calculated as: $\alpha_{tot} = 1/3\ (\alpha_{ss} + \alpha_{yy} + \alpha_{zz})$.

	α_{xx}	α_{yy}	α_{zz}	α_{tot}
PEN	90,7	36,2	12,9	46,6
PFP	94,8	38,1	13,0	48,7
HFDP	89,5	34,5	12,7	45,6
DAP	89,4	33,9	12,6	45,3
DHDAP	85,1	33,2	12,9	43,7
QUI	77,2	36,2	12,9	42,1
TET	65,2	39,1	13,0	39,1
QUA (diag.)	69,9	36,9	13,0	40,0
DNTT (diag.)	93,5	40,0	14,4	49,3

Quadrupole Moments:

Table ST5: Calculated quadrupole moments of all molecules in 10^{-34}Ccm^2. Magnitude of quadrupole moments given by: $\Theta_{tot} = \sqrt{3/2(\Theta_{xx}^2 + \Theta_{yy}^2 + \Theta_{zz}^2)}$

	Θ_{xx}	Θ_{yy}	Θ_{zz}	Θ_{tot}
PEN	4,9	4,0	-8,9	8,9
PFP	-3,7	-5,5	9,2	9,2
HFDP	9,4	-6,8	-2,6	9,7
DAP	10,7	-1,7	-9,0	11,5
DHDAP	-2,5	9,0	-6,5	9,3
QUI	16,3	-7,6	-8,8	16,3
TET	21,1	-15,3	-5,8	21,8
QUA (diag.)	17,7	-11,3	-6,4	17,9
DNTT (diag.)	-10,0	1,9	8,1	10,7

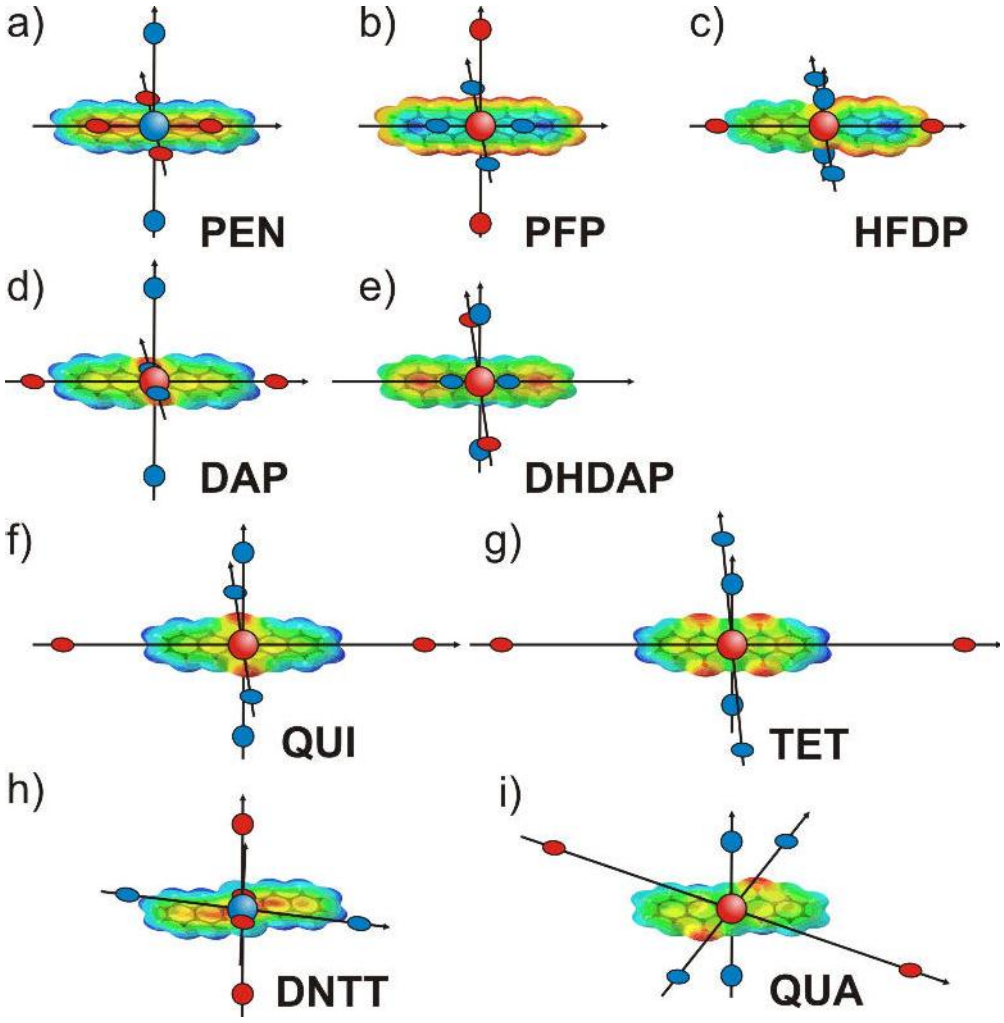

Figure S9: Visualization of quadrupole moments as point charge distributions together with MEPs of the various molecules. Positive charges are represented by red and negative one's by blue circles. The coordinate system is given by the eigenvectors of the corresponding matrix.

vdW-Volumes and Packing Coefficients

Van der Waals volumes V_{vdW} of molecules were calculated assuming spheres at all atomic positions with element specific vdW-radii and merging of all spheres. Following radii which are also used within the Crystal Explorer program [1] were applied throughout this work: H=1.09 Å; C=1.70 Å; N=1.55 Å; O=1.52 Å; F=1.47 Å. [2,3] For comparison the Hirshfeld volume V_H as computed with the Crystal Explorer is also listed. V_H is systematically larger than V_{vdW} but should exhibit the same trends. Packing coefficients C were calculated according to Kitaigorodskii [4] as $C = \frac{z \cdot V^{vdW}}{V_{cell}}$, where z denotes the number of molecules in the unit cell and V_{cell} is the unit cell volume.

Table ST6: Hirschfeld volumes V_H, molecular vdW volumes V_{vdW}, number of molecules z in the unit cell, unit cell volume V_{cell}, packing coefficient C.

	V_H (Å^3)	V_{vdW} (Å^3)	z	V_{cell} (Å^3)	C
PEN-C	339	245	2	692.38	0.71
PEN-S	338	244	2	685.49	0.71
PEN-TF	342	241	2	696.95	0.69
PFP-bulk	393	323	2	797.01	0.81
PFP-π	404	323	2	819.99	0.79
DNTT	376	269	2	767.71	0.70
QUA-α	340	251	1	347.27	0.72
QUA-β	331	249	2	674.50	0.74
QUA-γ	344	248	2	700.63	0.71
QUI	353	254	2	718.19	0.71
TET	373	267	1	379.41	0.70
DHDAP	327	236	2	667.85	0.71
DAP	327	240	2	667.78	0.72
HFDP	352	270	4	1433.75	0.75

[1] http://hirshfeldsurface.net
[2] A. Bondi, *J. Phys. Chem.*, 1964, **68**, 441.
[3] R.S. Rowland and R. Taylor, *J. Phys. Chem.*, 1996, **100**, 7384.
[4] A.I. Kitaigorodskii, *Acta. Cryst.*, 1965, **18**, 585.

Comparison of herringbone and slip-stacking of PFP

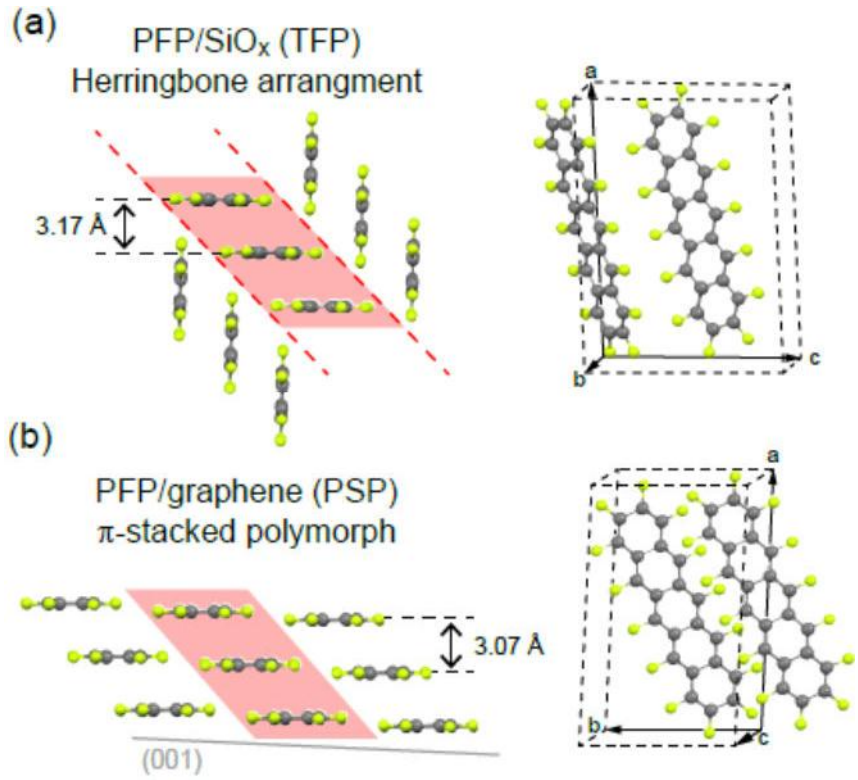

Figure S10: Comparison of the molecular arrangement in the two polymorphs of PFP: (a) herringbone arrangement of the bulk phase adopted on SiO_2 (top-view) and (b) slip-stacked arrangement of the π-stacked polymorph adopted in epitaxially grown PFP films (side-view) on graphite or graphene (taken from [1]). The pink region indicates the slip stacking that occurs in both in both polymorphs.

[1] I. Salzmann, A. Moser, M. Oehzelt, T. Breuer, X. Feng, Z.Y. Juang, D. Nabok, R.G. Della Valle, S. Duhm, G. Heimel, A. Brillante, E. Venuti, I. Bilotti, C. Christodoulou, J. Frisch, P. Puschnig, C. Draxl, G. Witte, K. Müllen and N. Koch, *ACS Nano*, 2012, **6**, 10874.